Journal of Power Sources 241 (2013) 744–750

Contents lists available at SciVerse ScienceDirect

Journal of Power Sources

journal homepage: www.elsevier.com/locate/jpowsour

Carbon paper substrate for silicon–carbon composite anodes in lithium-ion batteries

Q. Si [a,*], M. Matsui [a], T. Horiba [a], O. Yamamoto [a], Y. Takeda [a], N. Seki [b], N. Imanishi [a]

[a] Department of Chemistry for Materials, Graduate School of Engineering, Mie University, 1577 Kurimamachiya-cho, Tsu, Mie 514-8507, Japan
[b] Industrial Technology Center, Gifu Prefectural Government, 777 Maeno, Mino, Gifu 501-3716, Japan

HIGHLIGHTS

- Si-amorphous carbon (C)-carbon paper (CP) substrate for lithium secondary batteries.
- Direct deposition of Si/C composite on CP by pyrolysis of PVC mixed with Si.
- Initial Coulombic efficiency of 90% and initial capacity over 1700 mAh g^{-1}.
- Excellent cycleability with 70% capacity retention after 100 cycles.

ARTICLE INFO

Article history:
Received 28 March 2013
Received in revised form
10 May 2013
Accepted 20 May 2013
Available online 29 May 2013

Keywords:
Si/C composite electrode
Carbon paper substrate
Lithium-ion batteries
Initial Coloumbic efficiency
Cycle performance

ABSTRACT

We have developed a new Si-based anode for lithium secondary batteries consisting of a carbon paper substrate and Si/C composite deposited on it (Si/C/CP electrode). The Si/C composite was formed by pyrolysis of a slurry consisting of Si power and THF solution of PVC as the carbon precursor.

The electrode contains no additional conductive carbon and binder, which supports the tight contact among the Si particle, pyrolytic carbon and carbon paper. The Si/C/CP electrode with the three-dimensional carbon fiber framework of the carbon paper was also advantageous to absorb severe volume changes of silicon particles.

The electrode performance revealed that the Si/C/CP electrode prepared from the mixture of Si and PVC with the ratio of 10:90 by weight had a quite high initial capacity of 1720 mAh g^{-1} and initial Coulombic efficiency of 90%, and also exhibited excellent capacity retention with a reversible capacity of 1200 mAh g^{-1} even after 100 cycles.

1. Introduction

There has been continuous demand for high energy density lithium batteries toward long time operation of mobile electronics products such as laptop computers and mobile phones. And also of automotive and industrial applications whose introduction is recently expanding in a good pace. The energy density of the conventional Li-ion batteries with a graphite anode and a $LiCoO_2$ cathode has been improved for the past several decades [1]. Development of a high capacity electrode active material is one of the most effective ways to increase energy density of the battery. We focused on another important one, anode active material in this paper.

Sharma and Seefurth reported the formation of Li–Si alloys in high temperature cells operating at 400–500 °C [2]. It was described that the alloying proceeded stepwise as formation of $Li_{12}Si_7$, $Li_{14}Si_6$, $Li_{13}Si_4$, and $Li_{22}Si_5$ alloys. The study of the Li–Si binary system indicated that each silicon atom could accommodate 4.4 lithium atoms at most, which corresponds to specific capacity of 4200 mAh g^{-1} [2,3]. This is the highest among all elements to form alloy with lithium, and Li-extraction potential is lower than 0.5 V versus Li/Li^+ in average. In addition to its outstanding advantages, silicon is the second most abundant element on the earth. Because of these attributes, a great deal of attention has been paid to silicon as a lithium battery anode active material. However, the Si electrode showed a rapid capacity fading during cycling due to the large volume changes caused by Li-alloying and extraction, followed by the pulverization of the active materials and loss of electrical contact. The common strategy to improve the silicon-based

* Corresponding author. Tel.: +81 59 231 9420; fax: +81 59 231 9478.
E-mail addresses: siqin@chem.mie-u.ac.jp, hansiqin1014@yahoo.co.jp (Q. Si).

0378-7753
http://dx.doi.org/10.1016/j.jpowsour.2013.05.090

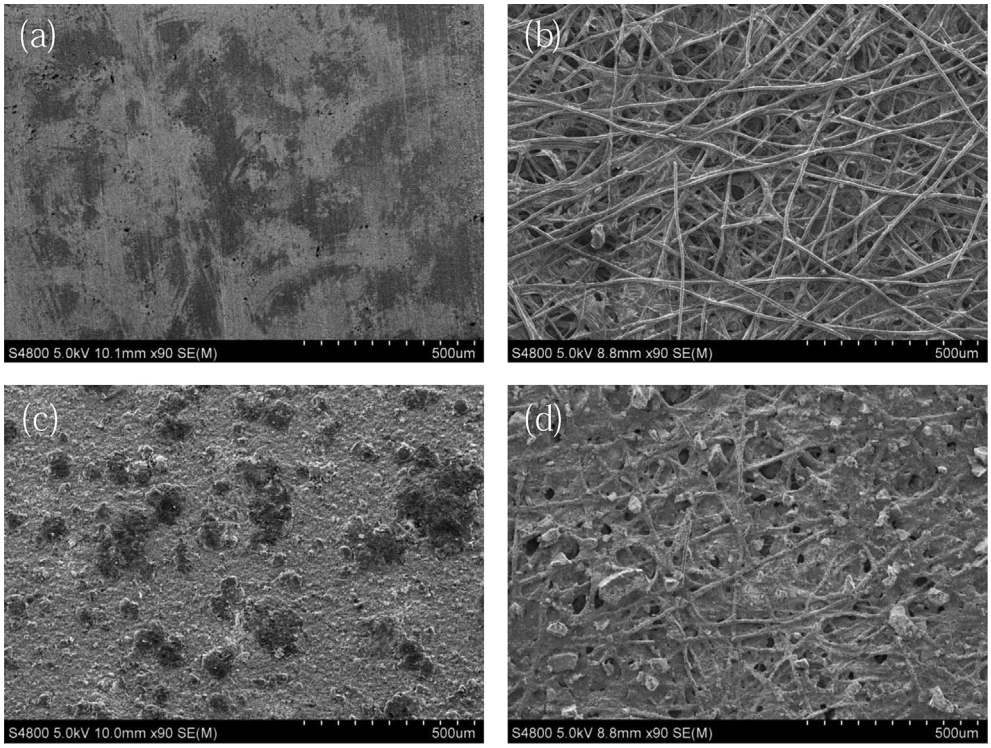

Fig. 1. SEM images of different electrode substrates and corresponding Si/C composite electrodes: (a) copper foil, (b) carbon paper, (c) Si/C composite electrodes on copper foil, and (d) Si/C composite electrodes on carbon paper.

electrode is to optimize the microstructure of the materials and the composition of the electrode, such as use of Si nano structured materials [4,5], preparation of Si-based composite [6–13] and modifying current collector [14–16].

Kim improved cycling performance of the silicon–graphite composite electrode by modifying the Cu foil surface [14]. Recently, Sa reported a high capacity Si–C composite electrode using Ni foam as the current collector [15]. Arbizzani used a carbon paper as the current collector for the tin anode and proved to be a good current collecting substrate to improve the cycling performance [17]. These results explicitly show that electrode substrate including the microstructure of the electrode is playing a very important role for alloying anode material accompanying large volume change. In all cases mentioned above, however, they introduced just new electrode substrates as the current collectors and there were no other improvement to prevent the fading of the conductive network during cycling.

Yang already reported on a Si/C composite electrode, comprising of Si particles with pyrolyzed carbon made from PVC (polyvinyl chloride) and graphite, and formed an electrode for lithium secondary batteries, which showed the initial Coulombic efficiency as high as 85% with a discharge capacity of 700 mAh g^{-1} [18].

We studied the Si/C composite electrode in more detail, and have presented that the Si/C composite electrode, comprising of Si particles with pyrolyzed carbon made from PVC, carbon black and PVdF (polyvinylidendifluoride) binder coated on a nickel foam current collector, showed initial Coulombic efficiency of 69% and a specific capacity of 920 mAh g^{-1}, in addition, stable cycling performance up to 40 cycles [19]. Introduction of carbon nano fiber (CNF) as the conductive material instead of carbon black and mixing it with Si powder and PVC before firing showed initial Coulombic efficiency of 73% and a specific capacity of 850 mAh g^{-1} [20]. In this electrode, we used not nickel foam but a copper foil as the electrode substrate. However, the copper foil as the electrode substrate for the Si/C anode showed that the active material mixture layer was not adhesive enough to be applied to prolonged lithiation/delithiation cycles.

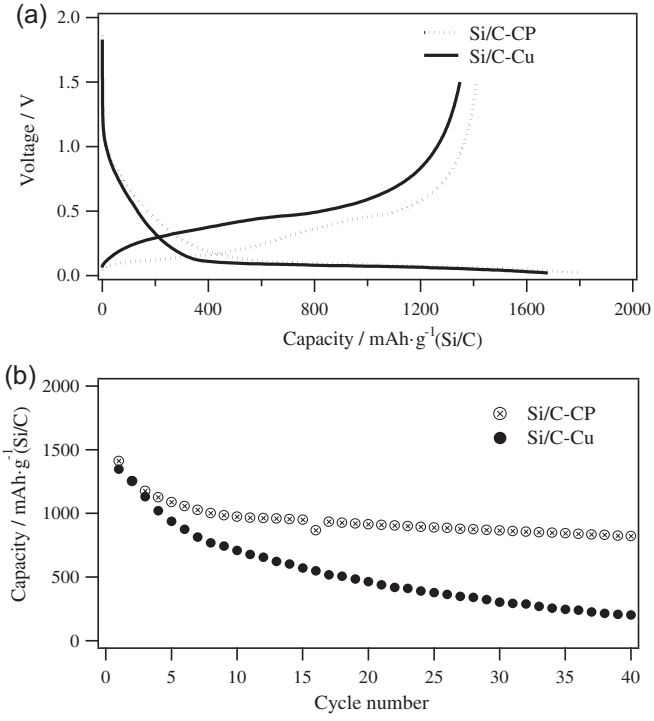

Fig. 2. Performance of Si/C composite electrodes with different substrates: (a) initial charge and discharge curves, and (b) cycling performance at 100 mA g^{-1}.

In this study, we will present a new Si/C composite anode using a carbon paper as a three-dimensional conductive substrate. The three-dimensional structure can incorporate the active material into the current collecting network, in particular, by the improved adhesion between carbon fiber of the paper and the Si/C composite deposited on it by the thermal decomposition of Si–PVC mixture. In this way we do not have to add a binder nor carbon conductive material. We will report some performance for the anode and discuss the reason of the results.

2. Experimental

2.1. Sample preparation

The Si/C composite was prepared according to the following procedure. A Si powder (0.5 μm, Kinsei Matec) and PVC (Sigma–Aldrich) with the ratio of 10:90 by weight were mixed in tetrahydrofuran (THF) and dried at 60 °C for 5 h. The mixture was then heated at 900 °C for 2 h in 2% H_2–Ar atmosphere [19,20]. The working electrodes which consisted of the Si/C composite active material, acetylene black, and PVdF with the ratio of 60:20:20 by weight was formed by painting the NMP (*n*-methyl pyrrolidone) slurry including the constituent materials onto copper foil or carbon paper, and drying at 80 °C for 1 h. The carbon paper was formed by carbonization of non-woven cloth made from natural cellulose fiber in inert atmosphere at 2600 °C, and had the thickness of 160 μm and area density of 48.2 gm^{-2}. The amount of Si in the Si/C with copper foil substrate (named as Si/C–Cu) and with the carbon paper substrate (named as Si/C–CP) were 0.4 mg cm^{-2} and 0.8 mg cm^{-2}, respectively.

A new composite electrode using the carbon paper substrate was prepared through another procedure: Si and PVC with the ratio of 10:90 were mixed in THF to prepare the slurry, and steeped the carbon paper in the slurry, after drying, heated at 900 °C for 2 h in 2% H_2–Ar. The electrode contained only the composite active materials without binder. The carbon paper used for this electrode was the same one as mentioned above. The weight ratio for Si/PVC/carbon paper is about 10/90/100, which changes to about 10/10/100 after pyrolysis. The amount of the Si/C active materials of the electrode (named as Si/C/CP) was 1.2 mg cm^{-2}. The ratio of Si:C in

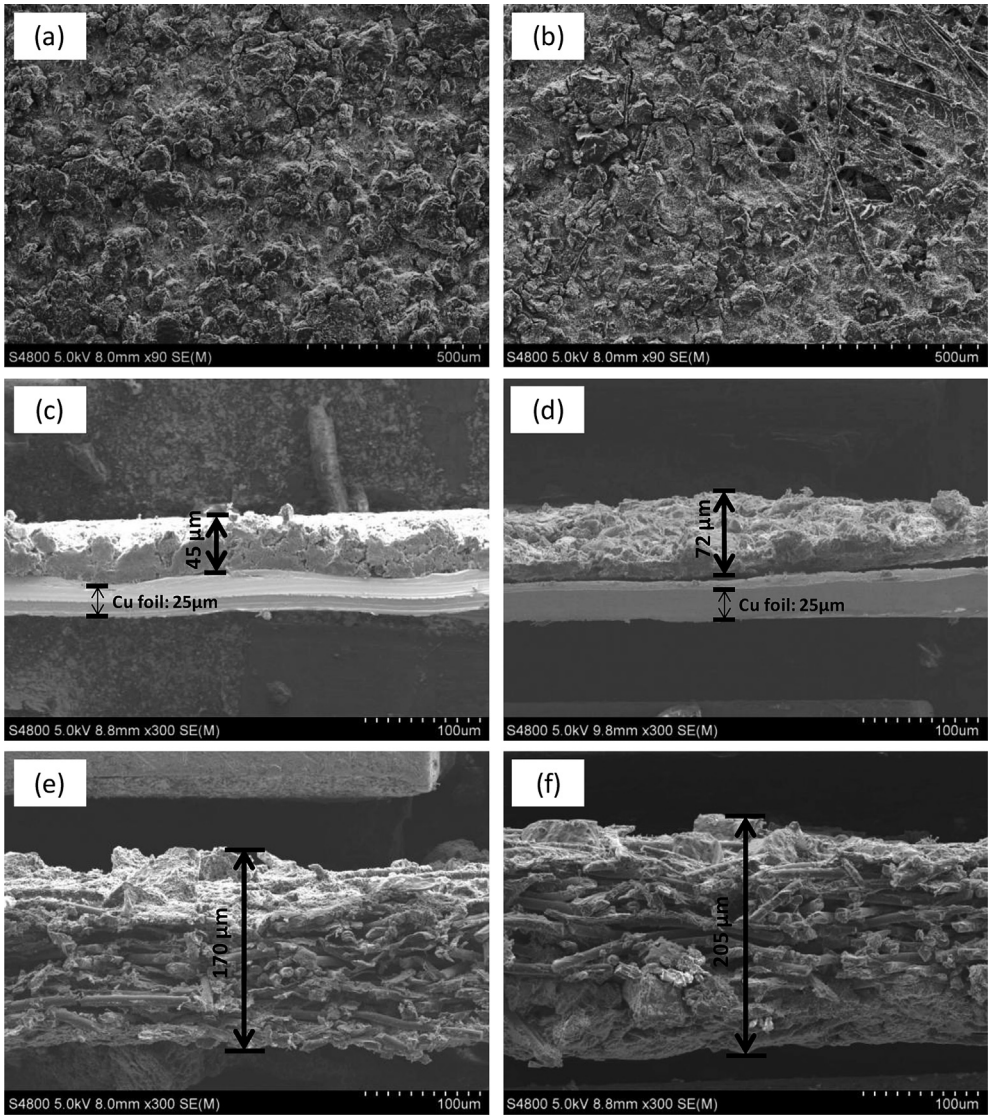

Fig. 3. Surface SEM images of the Si/C–Cu (a) the Si/C–CP (b) electrodes after 40 cycles and cross section SEM images of the Si/C–Cu (c, d) the Si/C–CP (e, f) electrodes before (c, e) and after (d, f) 40 cycles.

the Si/C active material is 1:1, that is 0.6 mg cm^{-2} Si and 0.6 mg cm^{-2} C.

The formed electrodes were cut into disks 12 mm in diameter, followed by drying at 120 °C under vacuum for 2 h. Two-electrode coin-type 2025 cells were used for the electrochemical measurements of the prepared electrodes. The coin cells were assembled in an argon glove box using 1 M $LiClO_4$ dissolved in ethylene carbonate (EC) and diethyl carbonate (DEC) mixture (1:1 in volume) as the electrolyte, a microporous polyolefin separator, and a metal lithium counter electrode. After cycling, the cells were carefully disassembled, and the electrodes were rinsed in dimethyl carbonate (DMC) to remove residual electrolyte and then dried at room temperature. The dried electrodes were cut with a razor blade to reveal the cross section for the observation.

2.2. Measurement

The charge–discharge characteristics were measured at room temperature between 0.02 V and 1.5 V at a constant current density of 100 mA g^{-1} with the rest time of 30 min after every charging and discharging, using Nagano BST 2004H, Japan. The electric current for the charge–discharge test and specific capacity were calculated based on the weight of not Si but Si/C composite. In this paper, the carbon paper showed a negligible small capacity at the same current density as that used in the charge–discharge test for the electrode.

For X-ray diffraction (XRD), we used a Rigaku RINT 2500/HLS diffractometer with Cu-Kα radiation. The morphology of the electrode substrates and electrodes was observed using scanning electron microscopy (SEM), Hitachi SEM S-4800.

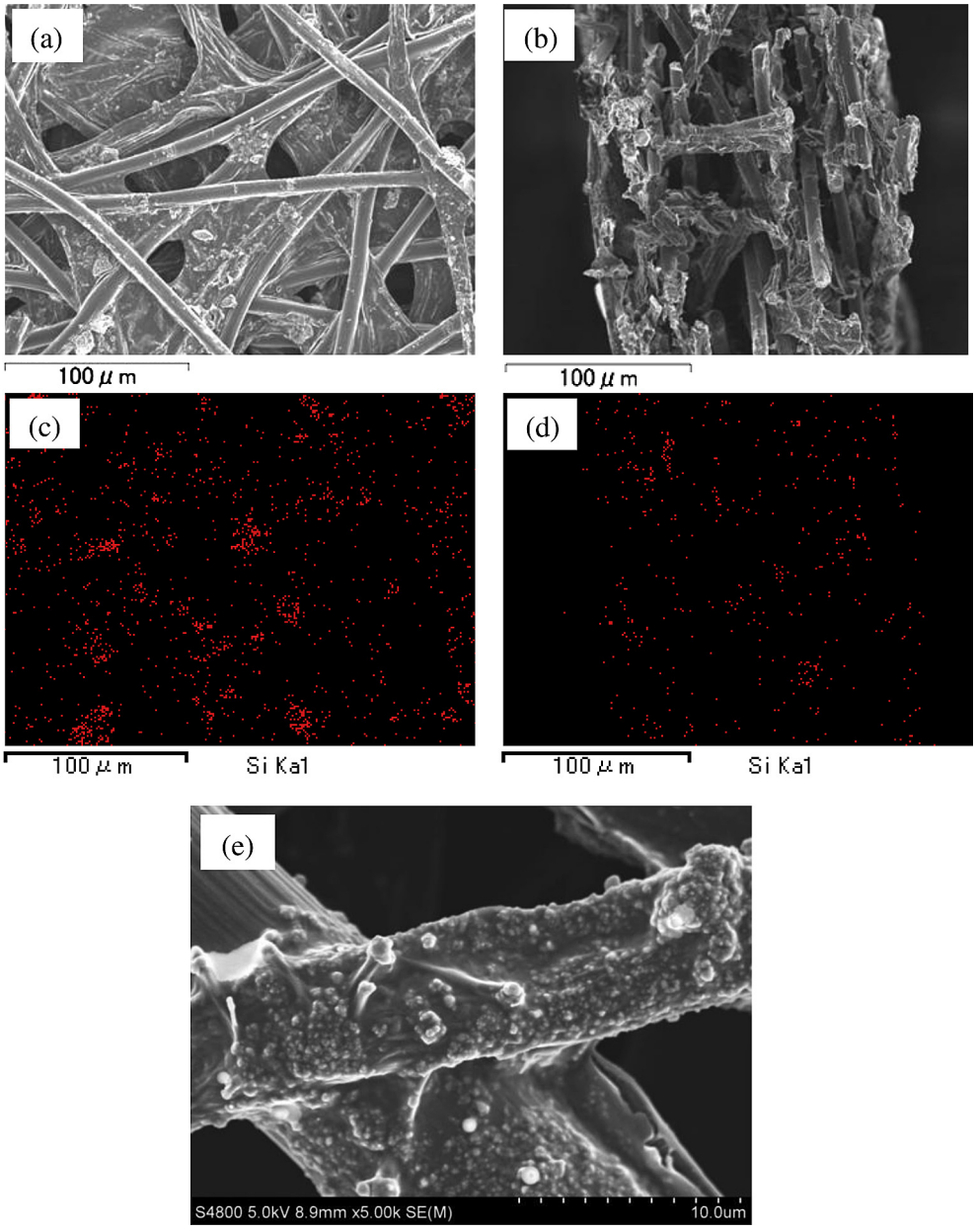

Fig. 4. SEM and EDX images of Si/C/CP electrode: (a) surface, (b) cross-section, (c) Si distribution of surface, (d) Si distribution of cross-section and (e) magnifying SEM image.

3. Results and discussion

3.1. Carbon paper substrate for Si/C composite electrode

Fig. 1 shows SEM images of the copper foil, carbon paper substrate and Si/C composite electrodes using them. Since PVdF itself does not have enough adhesion capability, the electrode could be easily peeled off from the Cu current collector. On the other hand, the carbon paper (Fig. 1(b)) shows a three-dimensional structure that enables to hold the Si/C composite active materials mixture as shown in Fig. 1(d). The Si/C composite active materials show a well-stuffed structure of the three-dimensional substrate.

Fig. 2 compares the voltage profiles of the first cycle and cycling stability of the Si/C composite electrodes with these two substrates. Fig. 2(a) shows that Si/C–CP improved discharge capacity compared with Si/C–Cu. The Coulombic efficiency for Si/C–CP reached 76%, which was almost the same as that for Si/C–Cu.

Fig. 2(b) shows a comparison of the cycling performance of the Si/C–Cu and the Si/C–CP. Both electrodes showed quick capacity drop during the initial 5–10 cycles. The Si/C–Cu initially showed 1350 mAh g^{-1} of specific capacity and then dropped to 940 mAh g^{-1} at the 5th cycle. The Si/C–CP also exhibited 1410 mAh g^{-1} of specific capacity and 1090 mAh g^{-1} at the 5th cycle. After the 5th cycle, these electrodes showed very different cycling stabilities. Compared with the specific capacity at 5th cycle, the Si/C–CP showed 75% of capacity retention at 40th cycle, while the Si/C–Cu showed continuous capacity loss during the 40 cycles.

In order to understand the improvement of cycling stability using the CP, the coin cells were disassembled after 40 cycles of the charge–discharge testing, and the electrode morphologies of these two electrodes were observed using SEM. Fig. 3(a) and (b) shows the surface SEM images of the Si/C–Cu and the Si/C–CP electrodes after the cycling respectively. Even though the as-prepared electrodes already shown in Fig. 1(c) and (d) had very different surface morphologies, the surface morphologies of both electrodes were very similar to each other after the cycling. The surface of the electrodes were very rough with several cracks, indicating significant volume expansion of the Si/C composite active materials. Fig. 3(c)–(f) shows the cross sectional SEM images of the Si/C–Cu and Si/C–CP electrodes before and after cycling. The Si/C–Cu electrode before cycling (Fig. 3(c)) has approximately 45 μm of thickness tightly adhered to the Cu foil, then the electrode expanded up to 72 μm (160% of original thickness) after the cycling as shown in Fig. 3(d). Notably the electrode paste partially delaminated from the Cu current collector. We speculate the significant volume expansion of the Si/C composite active materials initiated the partial delamination of the electrode paste resulting in the continuous capacity loss during the cycling. On the other hand, the thickness of the Si/C–CP electrode after cycling was 205 μm (Fig. 3(f)) corresponds to only 20% volume expansion of as-prepared electrode (Fig. 3(e)). In addition, the adhesion between the electrode paste and the carbon paper seems to maintain the good contact even after cycling. It is most likely due to the flexibility of the 3D structured CP, which absorbs the volume expansion of the

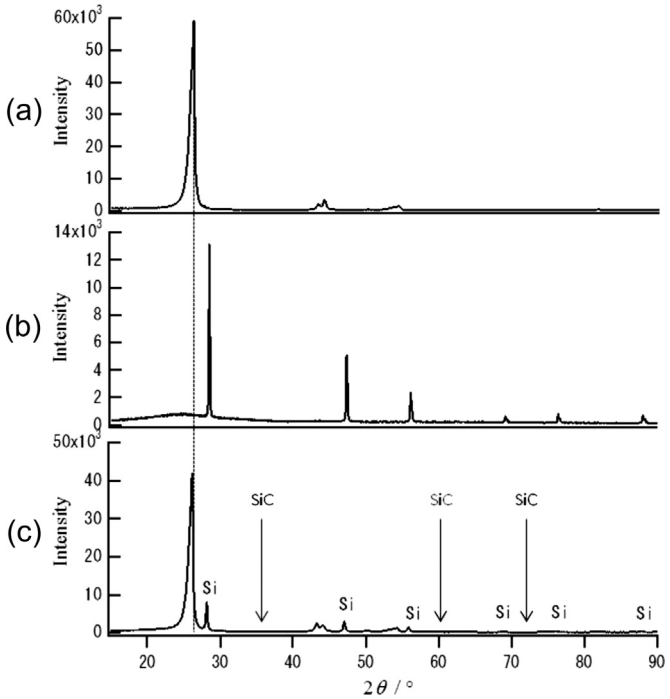

Fig. 5. XRD profiles: (a) carbon paper (CP), (b) Si/C composite, and (c) Si/C composite deposited into carbon paper substrate (Si/C/CP electrode).

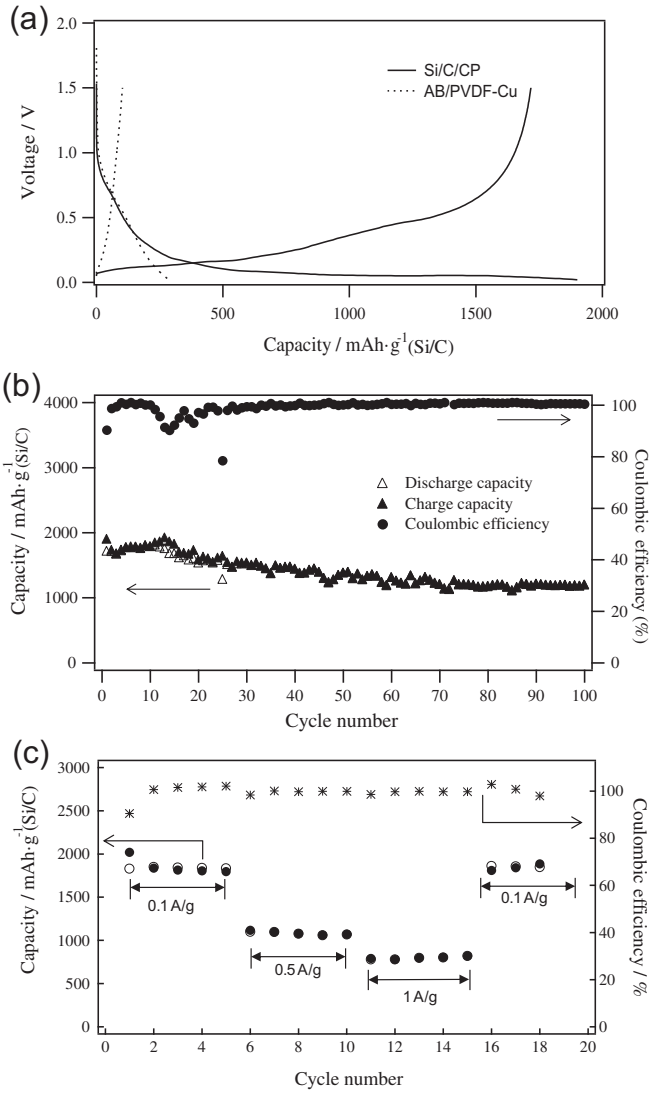

Fig. 6. Initial charge–discharge curves (a), charge–discharge cycling performance (b) and (c) rate performance of the Si/C/CP electrode.

Si/C composite active materials and maintains the electrical contact between the active materials and the CP substrate.

3.2. Directly deposited Si/C composite on carbon paper substrate

For the further improvement of the electrical contact between the Si/C composite active materials and the current collector, a direct deposition of Si/C composite onto the fiber of the carbon paper substrate was carried out. The direct deposited composite electrode (Si/C/CP) was prepared with following procedure. The carbon paper was steeped in the slurry of Si/PVC (10/90 by weight) dissolved in THF, after drying, heated at 900 °C under 2% H_2 in Ar flow. The electrode does not contain any binder and conductivity additive.

Fig. 4 displays SEM images of the binder-free Si/C/CP electrodes associated with the Si EDX mapping images. The surface SEM image of the Si/C/CP electrode shows that the Si/C composite active material was well-soaked in the fibers of the CP. The cross sectional image of the electrode shows that the Si/C composited active materials does not locate only at the surface of the electrode but in the middle of the electrode as shown in Fig. 4(b) and (d). A magnified SEM image of the Si/C/CP is shown in Fig. 4(e). The Si/C composite materials have attached on the surface of the carbon fiber of the CP, and the pyrolytic carbon seems to be working as a binder between Si and the carbon fiber of the CP.

Fig. 5 shows XRD patterns of the CP substrate (a), the Si/C composite active materials (b), and the Si/C/CP electrode (c). Fig. 5(a) shows the crystalline structure of CP and the main diffraction peaks at $2\theta = 26.5°$. Fig. 5(b) shows the XRD pattern of the Si/C composite active material. Since the diffraction pattern is in good agreement with that of Si overlapped with a broad peak around 26.5° of 2θ, the carbon matrix of the Si/C composite active materials consists of amorphous carbon. The XRD pattern of the Si/C/CP composite electrode shown in Fig. 5(c) is almost the same as the simple overlay of the XRD pattern of the carbon paper and the Si/C composite active material. In addition, there were no trace of a SiC or silicon oxides in Fig. 5(b) and (c). Therefore, we could verify that main compositions of Si/C composite were Si and amorphous carbon, and those of Si/C/CP were Si, carbon fiber graphite, and amorphous carbon.

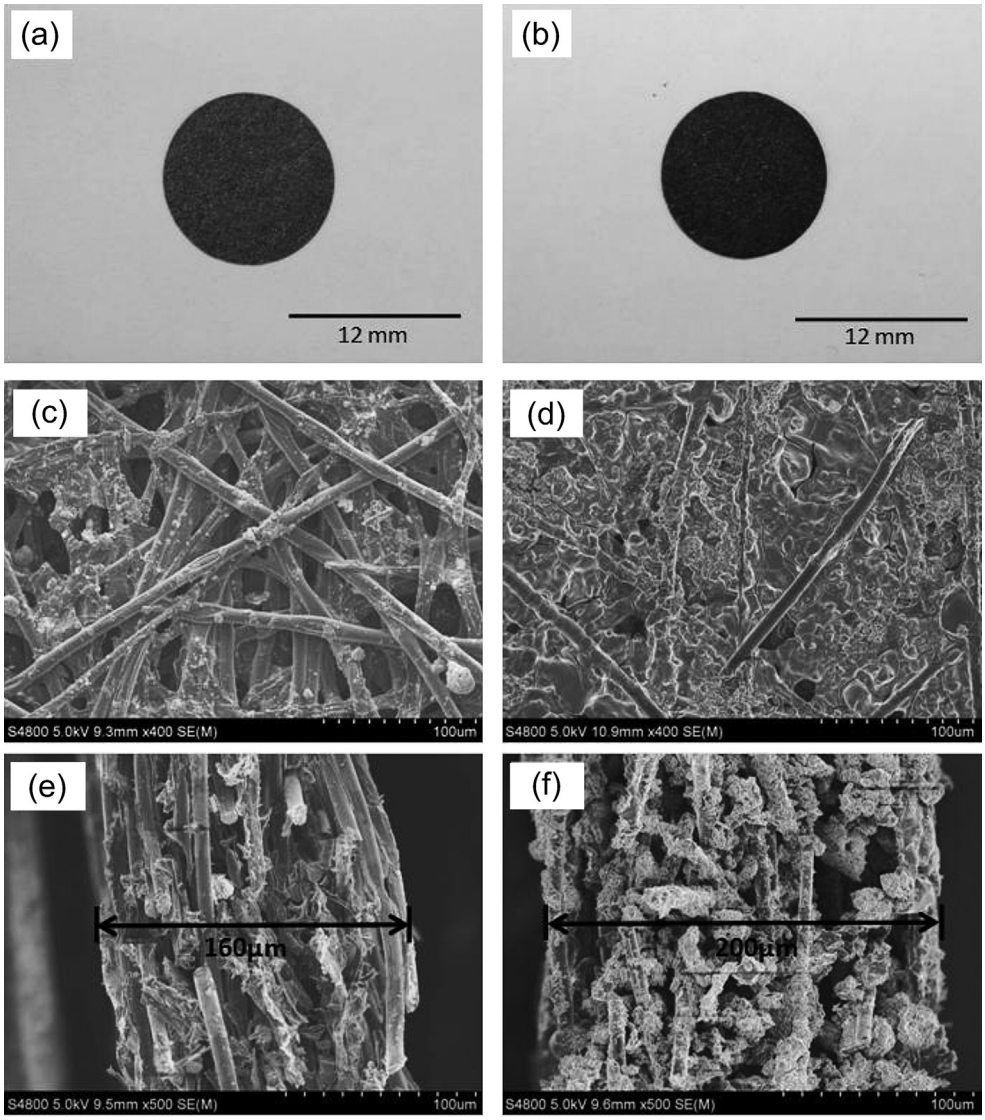

Fig. 7. Pictures of the Si/C/CP electrode before (a) and after (b) 100 cycles, surface SEM images of the Si/C/CP electrode before (c) and after (d) 100 cycles and cross section SEM images of the Si/C/CP electrodes before (e) and after (f) 100 cycles.

Fig. 6(a) shows initial charge–discharge curves of the Si/C/CP electrode. The initial discharge capacity of the Si/C/CP electrode was 1720 mAh g^{-1} while the charging capacity was 1900 mAh g^{-1} resulting in the 10% of the irreversible capacity in the initial cycle. The irreversible capacity of the Si/C/CP electrode was significantly lower than that observed in the case of the Si/C–CP electrode (24%). Since the irreversible capacity obtained just using an AB/PVdF coated electrode shown in Fig. 6(a) was approximately 65%, the lower irreversible capacity loss of the Si/C/CP electrode could be attributed to the free conductive additive in the electrode. Fig. 6(b) shows the cycling performance and Coulombic efficiency of the Si/C/CP electrode. The electrode showed a high reversible capacity of 1720 mAh g^{-1} and the reversible capacity of 1200 mAh g^{-1} was retained even after 100 cycles. The reversible capacity still remains 70% compared to the first cycle. Moreover, the Si/C/CP showed a high Coulombic efficiency of 90% from the first cycle and maintained 100% after 40 cycles.

The Si/C/CP maintained the high capacity even after the cycling process at higher rate as shown in Fig. 6(c). As the current densities increase from 0.1 to 0.5 to 1 Ag^{-1}, the electrode exhibits good capacity retention, as the specific capacities change from 1830 to 1100 to 800 mAh g^{-1}, respectively. Especially, it is noteworthy that when the current density returned to 0.1 Ag^{-1}, the specific capacity was restored to 1850 mAh g^{-1}.

There are two conceivable reasons to account for the enhanced electrochemical performance. First, an effectively conductive network could be constructed within the Si/C/CP electrode by the synergetic effect of pyrolytic carbon and carbon fibers of the carbon paper. The former sticks to Si particles and assists short-range conductivity for Si/C composite; the latter assists Si particles in long-range conductivity. Secondly, the pyrolytic carbon of the Si/C/CP electrode is expected to make the contact among the constituents tighter than does the PVdF binder of the Si/C–CP electrode.

Fig. 7(a) and (b) shows pictures of the Si/C/CP electrode before and after cycling. It is obvious that the Si/C/CP electrode has enough mechanical strength to maintain the original shape. The SEM images of the Si/C/CP electrode before and after 100 cycles are shown in Fig. 7(c)–(f). The Si/C/CP electrode before cycling (Fig. 7(c) and (e)) shows a well-defined three-dimensional structure with enough open pores in the electrode. After the cycling the open pore of the Si/C/CP electrode was filled with the expanded active materials as shown in Fig. 7(d). The comparison of the cross sectional SEM images of the Si/C/CP electrode before and after the cycling are shown in Fig. 7(e) and (f). The thickness of the Si/C/CP electrode expanded from 160 μm to 200 μm after the cycling. Even though the volume expansion rate of the Si/C/CP composite electrode was more than that of the Si/C–CP composite electrode, the cycling performance of the electrode was improved as discussed above. Therefore the effectively conductive network formed by the carbon fiber and the pyrolytic carbon matrix stuck to Si particles in the Si/C composite electrode. In addition, the Si/C/CP electrode was synthesized as a whole with structural integrity, and had suitable pore sizes and pore volume enough to absorb the Si volume change and retain the structural stability of the electrode.

The Si/C/CP electrode with the three-dimensional carbon framework by the carbon paper is also advantageous to absorb the severe volume changes of the silicon particles. This buffer function is expected to effectively mitigate the volume change of the electrode induced inside the electrodes during charging and discharging, and consequently to improve the cycleability and Coulombic efficiency of silicon-based anodes.

4. Conclusion

We have introduced a new electrode using a carbon paper substrate with three-dimensional carbon fiber network and Si/C composite deposited on it. The Si/C composite was formed by pyrolysis of a slurry consisting of Si power and THF solution of PVC as the carbon precursor. The electrode showed the initial Coulombic efficiency of 90% and the steady reversible capacity of 1200 mAh g^{-1} after 100 cycles. The improved performance of the electrode could be caused by a synergy effect of the conductive network of the carbon paper and the Si/C composite active materials. Future work should be focused to increase the capacity by effective packing of Si particles into the carbon paper without losing its conductive network along with the space for the particle to expand with holding enough amount of the electrolyte solutions in the electrode.

Acknowledgment

This research was sponsored by Japan Science and Technology Agency (JST) under the Adaptable and Seamless Technology Transfer Program (A-STEP).

References

[1] J.M. Tarascon, M. Armand, Nature 414 (2001) 359.
[2] R.A. Sharma, R.N. Seefurth, J. Electrochem. Soc. 123 (1976) 1763.
[3] B.A. Boukamp, G.C. Lesh, R.A. Huggins, J. Electrochem. Soc. 128 (1981) 725.
[4] H. Wu, Y. Cui, Nano Today 7 (2012) 414.
[5] Jeannine R. Szczech, S. Jin, Energy Environ. Sci. 4 (2011) 56.
[6] Y. Li, B.K. Guoa, L.W. Ji, Z. Lin, G.J. Xu, Y.Z. Liang, S. Zhang, O. Toprakci, Y. Hu, M. Alcoutlabi, X.W. Zhang, Carbon 51 (2013) 185.
[7] X. Zhou, A.M. Cao, L.J. Wan, Y.G. Guo, Nano Res. 5 (12) (2012) 845.
[8] Y. Hwa, W.S. Kim, S.H. Hong, H.J. Sohn, Electrochim. Acta 71 (2012) 201.
[9] M.S. Wang, L.Z. Fan, M. Huang, J.H. Li, X.H. Qu, J. Power Sources 219 (2012) 29.
[10] X.Y. Zhou, J.J. Tang, J. Yang, J. Xie, L.L. Ma, Electrochim. Acta 87 (2013) 663.
[11] F. Wang, S. Xu, S. Zhu, H. Peng, R. Huang, L. Wang, X. Xie, Paul K. Chu, Electrochim. Acta 87 (2013) 250.
[12] J. Q, H. Li, J.J. Henry Jr., S.K. Martha, N.J. Dudney, H. Xu, M. Chi, M.J. Lance, S.M. Mahurin, T.M. Besmann, S. Dai, J. Power Sources 198 (2012) 312.
[13] B.Y. Yu, L. Gu, C. Zhu, S. Tsukimoto, P.A. van Aken, J. Maier, Adv. Mater. 22 (2010) 2247.
[14] Y.L. Kim, Y.K. Sun, S.M. Lee, Electrochim. Acta 53 (2008) 4500.
[15] Q. Sa, Y. Wang, J. Power Sources 208 (2012) 46.
[16] J. Guo, A. Sun, C. Wang, Electrochem. Commun. 12 (2010) 981.
[17] C. Arbizzani, S. Beninati, M. Lazzari, M. Mastragostino, J. Power Sources 141 (2005) 149.
[18] J. Yang, B.F. Wang, K. Wang, Y. Liu, J.Y. Xie, Z.S. Wen, Electrochem. Solid-State Lett. 6 (8) (2003) A154.
[19] Q. Si, K. Hanai, N. Imanishi, M. Kubo, A. Hirano, Y. Takeda, O. Yamamoto, J. Power Sources 189 (2009) 761.
[20] Q. Si, K. Hanai, T. Ichikawa, A. Hirano, N. Imanishi, Y. Takeda, O. Yamamoto, J. Power Sources 195 (2010) 1720.